High-power passively Q-switched Nd:$GdVO_4$ laser with a reflective graphene oxide saturable absorber

Taijin Wang (汪太进), Jiang Wang (王 江), Yonggang Wang (王勇刚)*, Xiguang Yang (杨西光), Sicong Liu (刘思聪), Ruidong Lü (吕瑞东), and Zhendong Chen (陈振东)

School of Physics and Information Technology, Shaanxi Normal University, Xi'an 710119, China
**Corresponding author: chinawygxjw@snnu.edu.cn*

Received October 21, 2018; accepted December 20, 2018; posted online January 25, 2019

A single output Q-switched Nd:$GdVO_4$ laser with a reflective graphene oxide (GO) saturable absorber was demonstrated. The shortest pulse duration in the Q-switched laser is 115 ns, and the output power ranges from 1.23 W at 1.71 MHz to 2.11 W at 2.50 MHz when the pump power rises from 7.40 to 10.90 W with the utilization of GO Langmuir–Blodgett (LB) films based on the convenient and low-cost LB technique. To the best of our knowledge, it is the highest output power in a Q-switched laser with a GO saturable absorber.

OCIS codes: 140.3540, 140.3580, 160.4330.
doi: 10.3788/COL201917.020009.

Two-dimensional (2D) materials like graphene, black phosphorus, disulphide, topological insulators, bismuthene, and MXene have promising applications in lasers in the spectral range of 1–2 μm due to their remarkable photoelectric characteristics. As the first studied 2D materials, graphene and graphene-like 2D materials have a simple structure through convenient techniques compared with bismuthene, topological insulators, and MXene. It is more stable than black phosphorus without any protection under normal conditions[1–12].

It is reported that semiconductor materials such as GaAs[13] and semiconductor saturable absorber mirrors (SESAMs) have been adopted as Q-switched elements to generate laser pulses[14,15]. However, the laser pulses produced from GaAs absorbers are relatively unstable, while the SESAMs, as mature Q-switched elements, require complex fabrication and packaging.

Recently, graphene and graphene-like 2D materials, with the property of broadband saturable absorption[16–19], were composed of a simple structure through various convenient techniques and then used as the saturable absorber (SA) in passively Q-switched solid-state lasers[20,21]. The materials successfully used for the solid-state lasers were fabricated by one convenient technique called the vertical evaporation technique[22].

However, the qualities like thickness, flatness, and uniformity of the SA constructed by the convenient means cannot be controlled effectively. The Langmuir–Blodgett (LB) technique, a convenient and low-cost technique, was used to prepare an SA with better qualities compared with the SA made by the other methods. The LB technique can keep the thickness of the thin film within the nanometer level and the uniformity distribution of the nanomaterials under normal conditions[23], instead of magnetron sputtering[24] and ion beam aided evaporation[25] techniques with rigorous requirements in temperature and pressure, which may damage the material and film structures.

The reflective SAs have rarely been used as Q-switched elements to generate short pulses in a straight cavity compared with the transmissive SAs. The minimum length of the straight cavity is smaller than those of other types. By exploiting the straight cavity Q-switched solid-state lasers with the transmissive graphene oxide (GO) SA, 104 ns pulses and 1.22 W average output power with the slope efficiency of 17% were obtained[20].

In this Letter, the straight cavity Q-switched laser with a reflective GO SA fabricated by the LB technique has been constructed. The reflective GO SA with excellent performance in thickness and the uniformity of the nanomaterials was prepared by a convenient and low-cost technique. It was used as a Q-switched element in a straight cavity to generate pulses. The shortest pulse duration is 115 ns. The average output power and the slope efficiency are 2.11 W and 25.34%, respectively.

The liquid phase exfoliation (LPE) method is generally used to exfoliate the bulk 2D materials including graphene, black phosphorus, and transition metal dichalcogenides into nanoplates because of its simplicity and effectivity[26–28]. In this Letter, the method was used to exfoliate GO pieces purchased from XF NANO Inc. (Nanjing, China). The mixture of GO pieces and deionized water with a mass concentration of 2 mg/mL has been ultrasonicated for 24 h and then centrifuged for 20 min. The supernatant and methanol had been mixed at the volume ratio of 1∶4 to prepare the GO solution shown in Fig. 1(a). The GO LB films are to be produced after the ultrasonication of the acquired GO solution with 15 min.

The reflective GO SA shown in Fig. 1(b) is derived from the GO films adhering to the surface of a silver mirror through the LB technique. The silver mirror is a quartz plate coated with a silver film by the electron beam aided evaporation technique.

Figure 1(c) shows an LB system. In our experiment, a silver mirror was immersed in a trough containing

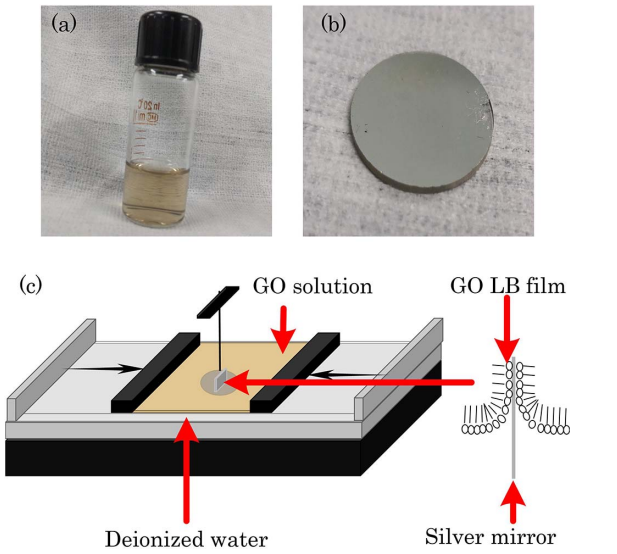

Fig. 1. (a) GO solution, (b) the reflective GO SA, and (c) the LB system.

200 mL deionized water with the pH of 7.0. The prepared GO solution was dipped and spread on the deionized water surface until the surface pressure reached 35 mN/m. The surface pressure was measured by a force transducer. When the surface pressure was stable, the silver mirror was pulled up slowly. At the same time, the GO solution was compressed by two mobile barriers controlled by a motor with the speed of 4.85 mm/min. When the silver mirror was pulled out of the liquid, the reflective GO LB films had been prepared. Finally, the silver mirror with GO LB films was dried at 80°C for 10 min to improve adhesion.

Figure 2(a) shows the scanning electron microscope (SEM) image of the GO LB films on the surface of the silver mirror. The thickness of the GO LB film was characterized by using an atomic force microscope (AFM), as displayed in Figs. 2(b) and 2(c). From Fig. 2(c), we found that the height of the LB film was calculated to be about 3–4 nm, demonstrating that the thickness of GO nanoplates on the film was relatively uniform. Figure 2(d) is the Raman spectrum of GO LB films. The two characteristic peaks are located at 1349 and 1595 cm^{-1}.

The chart in Fig. 3 presents the linear optical reflectivity curve of the reflective GO SA measured by a spectrophotometer (TU-1810). The reflectivity at 1064 nm is about 89.8%.

A self-made picosecond solid-state laser stimulated with the pulse of 40 ps and the repetition rate of 100 MHz at a wavelength of 1064 nm was used to measure the saturable absorption behavior of the reflective GO SA. The system is displayed in Fig. 4.

The output laser was divided into two laser beams after being focused by a convex lens. One was detected by a power meter as a reference light, while the other was reflected by the reflective GO SA and detected to confirm the nonlinear optical reflectivity of the reflective GO SA.

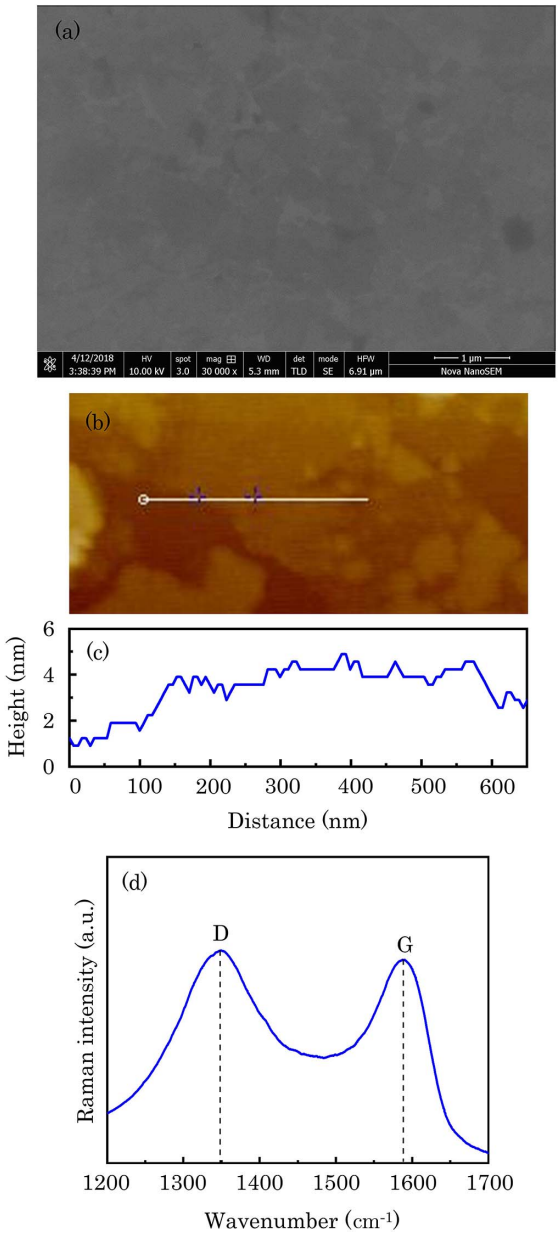

Fig. 2. (a) The scanning electron microscope image of the GO LB films, (b) the atomic force microscope image of the GO films, (c) the thickness of GO films, and (d) the Raman spectrum of the GO LB films.

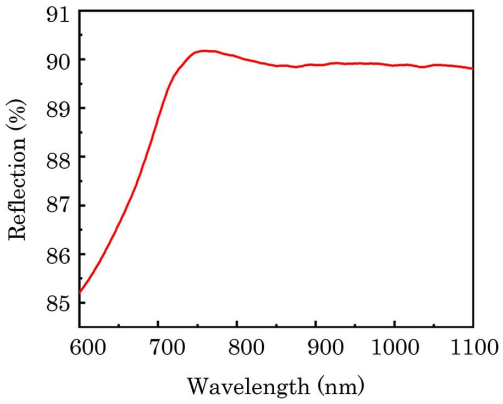

Fig. 3. Linear optical reflectivity curve of the reflective GO SA.

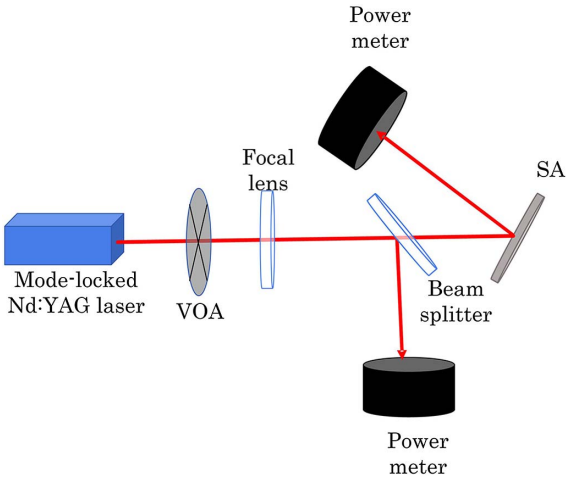

Fig. 4. Schematic diagram of experiment setup of nonlinear optical absorption measurement.

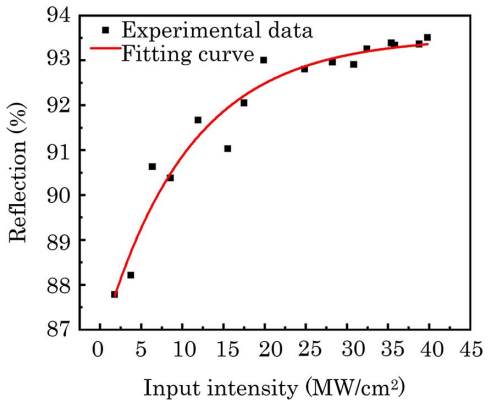

Fig. 5. Nonlinear optical reflectivity of the reflective GO SA.

The data of the nonlinear optical reflectivity of the reflective GO SA was recorded, as shown in Fig. 5, and curve fitted by the following equation[29]:

$$T(I) = 1 - \Delta T \cdot \exp\left(-\frac{I}{I_{\text{sat}}}\right) - T_{\text{ns}}, \tag{1}$$

where I, $T(I)$, I_{sat}, T_{ns}, and ΔT represent the input intensity, reflectivity, saturable intensity, non-saturable loss, and modulation depth, respectively.

Based on the fitting curve and the equation above, the corresponding values of the modulation depth (ΔT), saturable intensity (I_{sat}), and non-saturable loss (T_{ns}) are 6.8%, 10.6 MW/cm^2, and 6.5%.

The schematic setup is shown in Fig. 6. The pump beam came from a fiber-coupled laser diode (LD) with a central wavelength of 808 nm and then was focused into the Nd:$GdVO_4$ crystal with the beam waist of 400 μm by the 1∶1 coupling lens. There was an a-cut Nd:$GdVO_4$ crystal that was with the size of 3 mm × 3 mm × 5 mm and the Nd^{3+} doping concentration of 0.5 at. %. Both sides of its ends were coated with 808 and 1064 nm anti-reflection (AR) films. The gain crystal was maintained

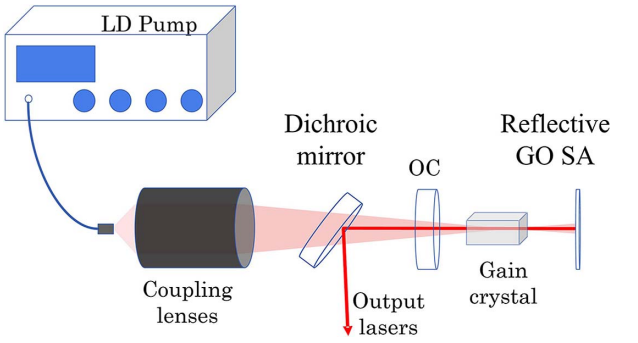

Fig. 6. Schematic setup of the passively Q-switched laser with reflective GO SA.

at 16°C by using water-cooled equipment. The output coupler (OC) ($R = 100$ mm) had a transmission of 7%. The OC was put at the side of the crystal towards the LD, and the reflective GO SA was put at the counterpart side. The length of the resonator was about 8 mm. The distance from the OC to the crystal is 1 mm, and the distance from the SA to the crystal is 2 mm. A dichroic mirror with 808 nm AR and 1064 nm high-reflection (HR) film was inserted into the cavity to output the laser.

Firstly, continuous wave (CW) operation was made. Then, the HR mirror was replaced by the reflective GO SA to generate a Q-switched wave (QW). The relationship between QW average output power and pump power in Fig. 7 is also obviously observable.

The Q-switching started when the pump power exceeded 7.40 W. The corresponding output power is 1.23 W. The repetition rate is 1.70 MHz, and pulse duration is 186 ns. Figure 8 shows the evolutions of the pulse repetition rate and the pulse duration with the pump power. These data were measured by a digital oscilloscope (Rohde & Schwarz, RTO1014) with a photodetector (Thorlabs, DET10A/M). The output power is 2.11 W when the pump power was adjusted to 10.9 W.

Figure 9 shows the different pulse trains when the pump powers were 8.60, 9.60, and 10.90 W, corresponding to the repetition rates of 1.72, 1.85, and 2.50 MHz.

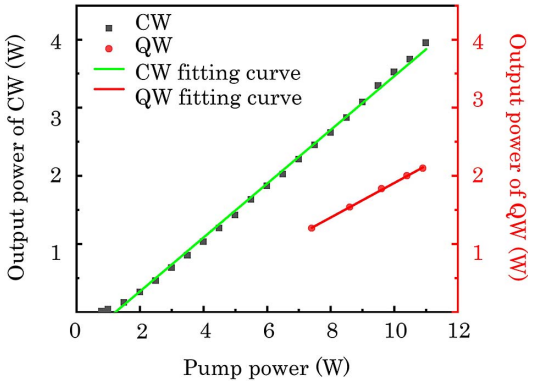

Fig. 7. Average output power of CW and QW versus the pump power.

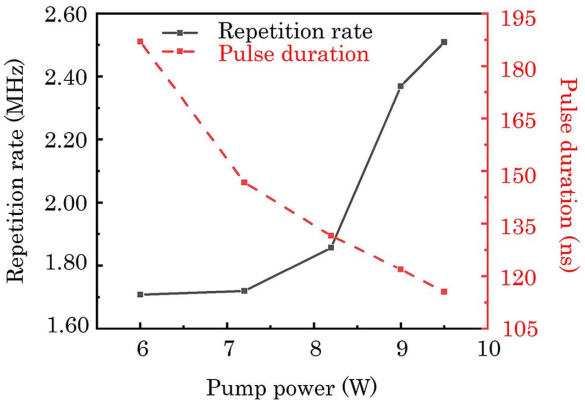

Fig. 8. Evolutions of the pulse repetition rate and the pulse duration with pump power.

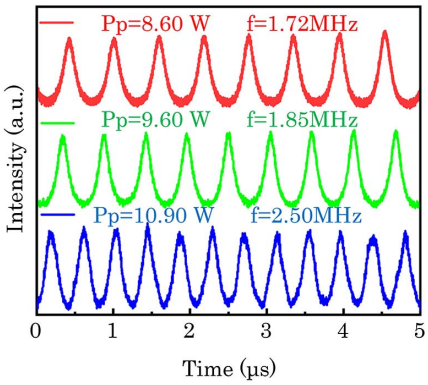

Fig. 9. Pulse trains of Q-switched lasers under different pump powers.

It was demonstrated that the repetition rate got higher when the pump power increased. The slight jitter of the pulse was caused by the degeneration of SA due to heat accumulation when the pump power was up to 10.90 W. The pulse duration of 115 ns is displayed in Fig. 10.

The QW spectrum shown in Fig. 11 was measured by an optical spectrum analyzer (YOKOGAWA, AQ6370D). The central wavelength (λ_c) was 1063.20 nm with the 3 dB bandwidth of 0.14 nm.

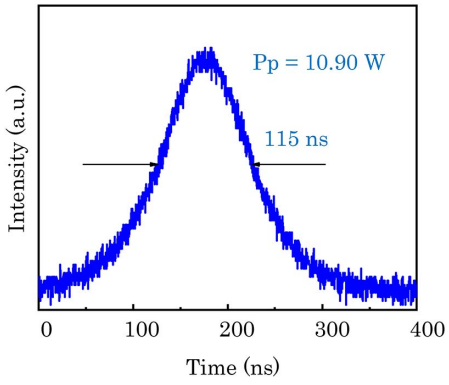

Fig. 10. Single pulse under the pump power of 10.90 W.

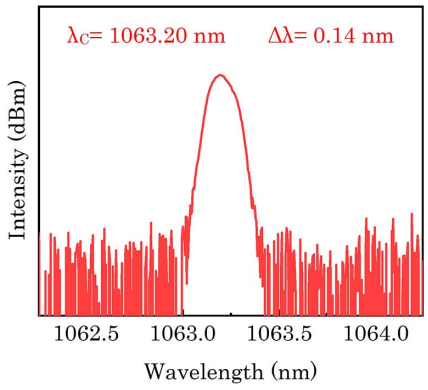

Fig. 11. QW spectrum.

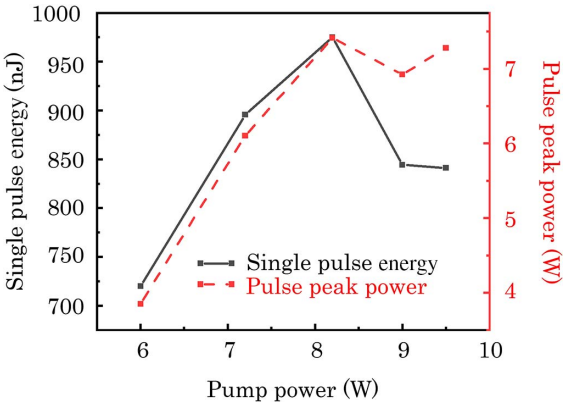

Fig. 12. Evolutions of the single pulse energy and the pulse peak power with the pump power.

Figure 12 shows the single pulse energy and peak power versus the pump power. The highest pulse peak power is 7.42 W, and the largest single pulse energy is 975 nJ.

In conclusion, a kind of reflective GO SA with excellent performance in thickness and the uniformity of the nanomaterials was fabricated through the LB technique and used in linear cavity solid-state Q-switched lasers. The highest Q-switched output power is 2.11 W, the shortest pulse duration is 115 ns, and the highest repetition rate is 2.50 MHz. To the best of our knowledge, it is the highest output power in a Q-switched laser with GO SA.

This work was financially supported by the Central University Special Fund Basic Research and Operating Expenses (No. GK201702005), the Natural Science Foundation of Shaanxi Province, China (No. 2017JM6091), and the Fundamental Research Funds for the Central Universities (No. 2017TS011).

References

1. F. Bonaccorso, Z. Sun, T. Hasan, and A. C. Ferrari, Nat. Photon. **4**, 611 (2010).
2. H. Zhang, J. Liu, Z. Chu, and Z. Guo, Opt. Mater. Express **6**, 2374 (2016).

3. X. Wang, Z. Wang, Y. Wang, L. Li, G. Yang, and J. Li, Chin. Opt. Lett. **15**, 011402 (2017).
4. H. Zhang, J. Xu, X. Hu, Y. Xue, Z. Xie, and Z. Ye, Chin. Opt. Lett. **16**, 102401 (2018).
5. L. Li, Y. Yu, G. J. Ye, Q. Ge, X. Ou, H. Wu, D. Feng, X. C. Hui, and Y. Zhang, Nat. Nanotechnol. **9**, 372 (2014).
6. J. Ma, S. Lu, Z. Guo, X. Xu, H. Zhang, D. Tang, and D. Fan, Opt. Express **23**, 22643 (2015).
7. Z. Guo, H. Zhang, S. Lu, Z. Wang, S. Tang, J. Shao, Z. Sun, H. Xie, H. Wang, X. F. Yu, and P. K. Chu, Adv. Funct. Mater. **25**, 6996 (2016).
8. X. Wang, Y. Wang, L. Duan, L. Li, and H. Sun, Opt. Commun. **367**, 234 (2016).
9. Y. Chen, C. Zhao, S. Chen, J. Du, P. Tang, G. Jiang, H. Zhang, S. Wen, and D. Tang, IEEE J. Sel. Top. Quantum Electron. **20**, 315 (2014).
10. X. Jiang, S. Gross, H. Zhang, Z. Guo, M. J. Withford, and A. Fuerbach, Annal. Phys. **528**, 543 (2016).
11. L. Lu, Z. Liang, L. Wu, Y. X. Chen, Y. Song, S. C. Dhanabalan, J. S. Ponraj, B. Dong, Y. Xiang, F. Xing, D. Fan, and H. Zhang, Laser Photon. Rev. **12**, 1700221 (2018).
12. X. Jiang, S. Liu, W. Liang, S. Luo, Z. He, Y. Ge, H. Wang, R. Cao, F. Zhang, Q. Wen, J. Li, Q. Bao, D. Fan, and H. Zhang, Laser Photon. Rev. **12**, 1700229 (2017).
13. A. L. Gaeta and T. T. Kajava, Opt. Lett. **21**, 1244 (1996).
14. B. Braun, F. X. Kärtner, G. Zhang, M. Moser, and U. Keller, Opt. Lett. **22**, 381 (1997).
15. E. Mehner, B. Bernard, H. Giessen, D. Kopf, and B. Braun, Opt. Lett. **39**, 2940 (2014).
16. X. Li, Y. Tang, Z. Yan, Y. Wang, B. Meng, G. Liang, H. Sun, X. Yu, Y. Zhang, X. Cheng, and Q. J. Wang, IEEE J. Sel. Top. Quantum Electron. **20**, 441 (2014).
17. F. Zhao, Y. Wang, Y. Wang, H. Wang, and Y. Cai, Chin. Opt. Lett. **15**, 101402 (2017).
18. H. Zhang, D. Tang, R. J. Knize, L. Zhao, Q. Bao, and K. P. Loh, Appl. Phys. Lett. **96**, 51 (2010).
19. L. Jiao, L. Zhang, X. Wang, G. Diankov, and H. Dai, Nature **458**, 877 (2009).
20. Y. Wang, H. Chen, X. Wen, W. Hsieh, and J. Tang, Nanotechnology **22**, 455203 (2011).
21. X. Li, J. Xu, Y. Wu, J. He, and X. Hao, Opt. Express **19**, 9950 (2011).
22. H. Shimoda, S. J. Oh, H. Z. Geng, R. J. Walker, X. B. Zhang, L. E. McNeil, and O. Zhou, Adv. Mater. **14**, 899 (2002).
23. Q. Zheng, J. Wang, Y. Wang, and Z. Chen, Opt. Mater. Express **8**, 3176 (2018).
24. I. M. Ioan, X. Sun, and B. Luan, Can. J. Chem. **93**, 160 (2015).
25. S. Fujimori, T. Kasai, and T. Inamura, Thin Solid Films **92**, 71 (1982).
26. Y. Yu, Z. Han, Y. Zhang, B. Dong, A. Kong, and Y. Shan, Sci. Adv. Mater. **8**, 1321 (2016).
27. J. Li, H. Luo, B. Zhai, R. Lu, Z. Guo, H. Zhang, and Y. Liu, Sci. Rep. **6**, 30361 (2016).
28. A. Shmeliov, M. Shannon, P. Wang, J. S. Kim, E. Okunishi, P. D. Nellist, K. Dolui, S. Sanvito, and V. Nicolosi, ACS Nano **8**, 3690 (2014).
29. H. Liu, Z. Sun, X. Wang, Y. Wang, and G. Cheng, Opt. Express **25**, 6244 (2017).